Academic Journal of Science and Technology
ISSN: 2771-3032 | Vol. 15, No. 2, 2025

Research on the Effect of the Sequence of Exterior Concrete Placement on the Stability of Reinforced Concrete Arches with Rigid Skeleton

Yi Cai

College of Civil Engineering, Lanzhou Jiaotong University, Lanzhou 730070, China

Abstract: In the process of casting concrete in the outer package of reinforced concrete arch bridge with strong skeleton, the force state of the main arch ring will be constantly changed with the advancement of concrete casting, and this dynamic load distribution makes the mechanical properties of the main arch ring extremely complicated. It is a key issue in the construction of reinforced concrete arch bridges with strong skeleton to study the influence of different pouring sequences on the linearity and stability of the arch ring. This paper takes a reinforced concrete arch bridge with strong skeleton on the Sichuan-Tibet line as the engineering background, and simulates the influence of different pouring sequences of exterior concrete on the stability of the strong skeleton concrete arch ring. Based on the optimal working surface (eight working surfaces) and the optimal pouring method (ring-segmented pouring), 24 first pouring schemes are numerically simulated, and the optimal location of the first pouring section is determined through the analysis and comparison of stability and deflection analyses. The study shows that the first-order flexural modal coefficient of Scheme 4 (simultaneous casting of 1-1, 3-1, 5-1 and 7-1 bottom slabs) reaches 22.51, which is the highest value of all the schemes, indicating that its ability to resist instability is significantly enhanced. In addition, the deflections of scheme 4 in all critical sections are at the lowest level, and the maximum deflection is 86.9% lower than the worst scheme, and the distribution shows a gradual growth characteristic, which avoids the risk of local abrupt changes in the high deflection scheme.

Keywords: Rigid Skeleton Main Arch Circle; Pouring Working face; Sequence of Pouring Concrete for Outsourcing; Stability; Nonlinear analysis.

1. Introduction

Bergmeister K, Capsoni A and Corradi L[1] investigated the effect of deck girder slenderness on transverse buckling loads of arch steel bridges. Fangcun Song and Hu Jia[2] numerically simulated the linear elastic response and geometrically nonlinear load carrying performance of steel arch bridges by constructing a three-dimensional solid finite element model with parametric analysis method through engineering examples. Shangying Xie[3], Dongsheng Qian and Anbang Gu[3] studied the stability of a 180m span steel pipe concrete strong skeleton arch bridge, and the analysis showed that the influence of nonlinearity, especially the material nonlinearity, should be considered when the stability calculation of the large span steel pipe concrete strong skeleton arch bridge is carried out. Gangruo Wu[5] and Bingcheng Yang[6] establish finite element models of Pingyikou Bridge and Ziyang Hanjiang Bridge based on ANSYS to reveal the dynamic folding mechanism of the stiffness of the stiffness skeleton under the action of double nonlinear coupling, and the study shows that the construction of the split ring enhances the sensitivity to material nonlinearity by 18.7%, and the geometrical nonlinear increment induced by segmental construction is exponentially correlated with the span diameter. Chen Xiaobo[7] found that the sequence of concrete filling in the steel pipe had little effect on the stress of the stringers through the calculation and analysis of the construction process, and the three-ring pouring scheme for the outer concrete could avoid the appearance of tensile stress. The stability coefficients of the maximum cantilever stage of the steel pipe and after pouring concrete are more than 4, which meet the specification requirements. This kind of structural system with compression bending force as the main force, its stable bearing capacity is significantly affected by the construction timing effect. Therefore, it is important to study the stability of the main arch ring during the casting of the outer concrete.

2. Model

2.1. Establishment of foundation pit model

The construction phase analysis of the main arch ring of the strong skeleton was simulated using Midas Civil finite element computational simulation software. Among them, the main arch ring of the strong skeleton and the outsourced concrete are simulated by beam unit, and the steel pipe concrete is simulated by joint section method, and the beam unit of the strong skeleton and the beam unit of the outsourced concrete are coupled with each other through the common unit section, and the whole model of the main arch ring of the strong skeleton contains 460 nodes and 1588 units, and the main arch ring of the strong skeleton is simulated by Midas Civil finite element calculation and simulation software. The grid division is shown.

Figure 2.1 Finite element calculation model diagram of the main arch ring of the strong skeleton

The outer concrete was poured in sections and rings as shown below:

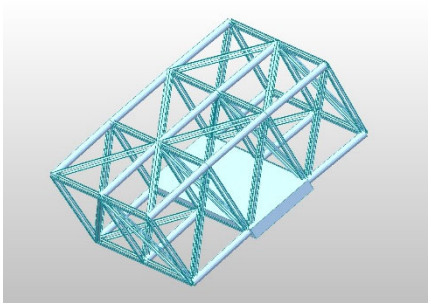

Figure 2.2 Bottom slab pouring

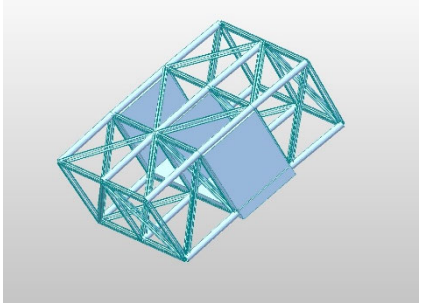

Figure 2.3 Web casting

Eight working faces means that the outer concrete of the main arch ring is divided into 8 working faces, and each working face is divided into 3 small sections, with a total of 24 working sections, and the pouring method is divided into ring section pouring and section direct pouring, and the pouring sequence is symmetrical pouring, as shown in Fig. 2.4 below, and the construction program is shown in Table 4.3 below.

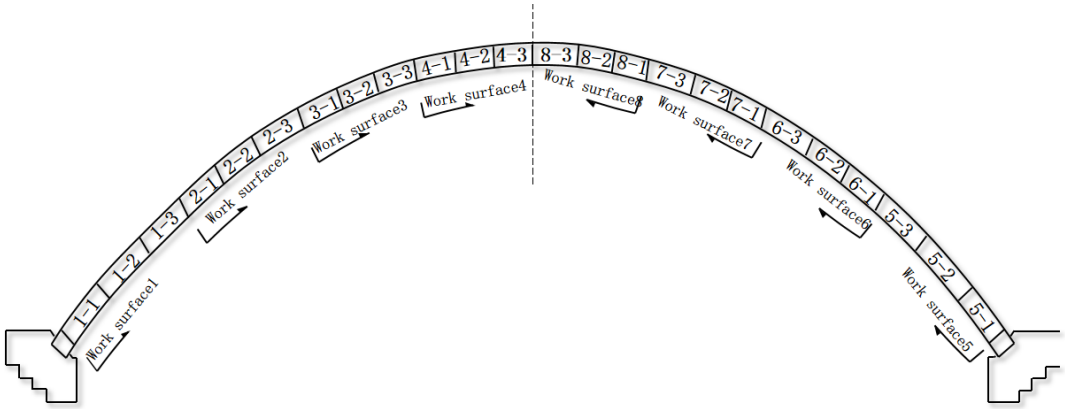

Figure 2.4. Division of eight working sections

2.2. Selection of finite element support scheme

The study will simulate the symmetrical pouring from 4 working sections simultaneously, and select the optimal first pouring section by comparing the deflection and stability of the arch ring, listing 24 pouring schemes in the following Table 2.1, and deriving the optimal first pouring section by simulating multiple pouring schemes.

Table 2.1 First pour program

Program	Casting section	Program	Casting section
1	1-1、2-1、5-1 and 6-1	13	2-1、3-2、6-1 and 7-2
2	1-2、2-2、5-2 and 6-2	14	2-1、3-3、6-1 and 7-3
3	1-3、2-3、5-3 and 6-3	15	2-2、3-1、6-2 and 7-1
4	1-1、3-1、5-1 and 7-1	16	2-2、3-3、6-2 and 7-2
5	1-2、3-2、5-2 and 7-2	17	2-3、3-1、6-3 and 7-1
6	1-3、3-3、5-3 and 7-3	18	2-3、3-2、6-3 and 7-2
7	1-1、4-1、5-1 and 8-1	19	2-1、4-1、6-1 and 8-1
8	1-2、4-2、5-2 and 8-2	20	2-2、4-2、6-2 and 8-2
9	1-3、4-3、5-3 and 8-3	21	2-3、4-3、6-3 and 8-3
10	2-1、3-1、6-1 and 7-1	22	3-1、4-1、7-1 and 8-1
11	2-2、3-2、6-2 and 7-2	23	3-2、4-2、7-2 and 8-2
12	2-3、3-3、6-3 and 7-3	24	3-3、4-3、7-3 and 8-3

3. Analysis of the First Pouring of Outsourced Concrete Working Face

3.1. Stability analysis

In order to study the different pouring sequences of the eight working faces, the first pouring section should be determined, and the first pouring section should be selected at the location where the structural stress is more uniform and has less influence on the overall stability, so as to avoid the structural instability due to the concentration of local stress, and to effectively control the position of the main arch ring line shape, so as to make sure that the line shape of the subsequent pouring section is in accordance with the design requirements. The construction progress should also be considered to ensure that the subsequent casting section can be carried out according to the plan to avoid the overall progress being affected by the delay in the construction of the first casting section. After determining the first pouring section, different pouring sequences for the 8 working faces are further studied, such as from the top of the arch to the foot of the arch, from the foot of the arch to the top of the arch, or alternating pouring, etc. The optimal pouring sequence is determined through numerical simulation to ensure that the line shape and stability of the main arch ring meets the design requirements. Table 3.1 below shows the first-order buckling modal coefficients for linear buckling analysis for each of the 24 casting scenarios simulated separately, and Figure 3.1 shows the first-order modal coefficients for each scenario for the first casting.

Table 3.1 First-order flexural modal coefficients for each scenario of the first casting

Program	Buckling mode coefficient	Program	Buckling mode coefficient	Program	Buckling mode coefficient
1	12.83	9	13.92	17	16.47
2	13.98	10	18.07	18	9.34
3	18.09	11	15.61	19	8.63
4	22.51	12	11.54	20	10.31
5	19.37	13	17.89	21	6.43
6	15.25	14	13.12	22	7.00
7	14.41	15	17.14	23	6.56
8	13.41	16	9.87	24	6.20

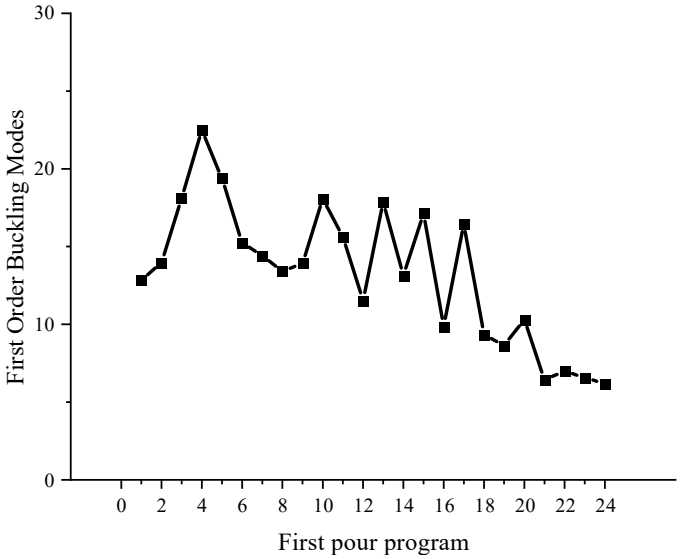

Figure 3.1. First-order flexural modal coefficients for each scenario of the first casting

As can be seen from Table 3.1 and Figure 3.1, Option 4 has the highest value of 22.51, which is significantly higher than the other options, and therefore can be considered as the optimal solution for placing the exterior concrete. The corresponding pouring location of this scheme is "simultaneous pouring of 1-1, 3-1, 5-1 and 7-1 base slabs". The first-order flexural modal coefficient is an important index for evaluating the ability of the structure to resist deformation under stress. The coefficient for Option 4 (22.51) is much higher than the average of 24.24, indicating that this pour sequence provides the best structural stability. The pouring locations "1-1, 3-1, 5-1 and 7-1" for option 4 can be found to show a balanced distribution of these locations. This distribution may have resulted in more uniform shrinkage stresses after the concrete was poured, reducing stress concentrations within the structure. The locations chosen for Option 4 may have created a more reasonable stress transfer path, which contributes to the uniform distribution and transfer of structural forces. In contrast, the first-order flexural modal coefficients of Option 19 (18.63), Option 22 (17.00), Option 23 (14.56), and Option 24 (16.20) are lower, indicating that the structural stability of these pouring options is relatively poor, and all of them have a pouring section at the pouring location close to the vault.

In summary, the first casting scheme is to cast 1-1, 3-1, 5-1 and 7-1 bottom slabs at the same time, and Figures 3.2 and

3.3 show the first-order and second-order flexural modes of the main arch ring during the first casting, respectively.

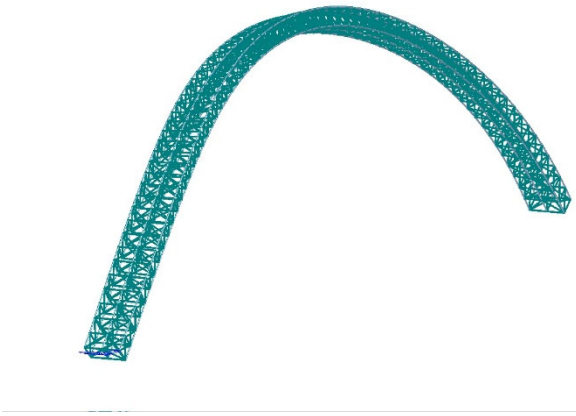

Figure 3.2. First-order flexural modes

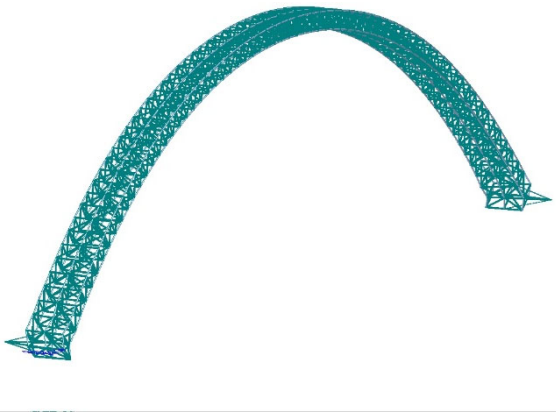

Figure 3.3. Second-order flexural modes

3.2. Iinear analysis

Through the Midas Civil software simulated the first time of outsourcing concrete bottom slab casting of 24 casting schemes, respectively, the foot of the arch, half-arch 1/8 cross-section, half-arch 1/4 cross-section, half-arch 3/8 cross-section, half-arch 1/2 cross-section, as well as the top of the arch cross-section of the deflection at the comparative analysis combined with the deflection value of the extreme value, the sum, the average value and distribution of the equilibrium, the comprehensive screening out of the optimal casting scheme. Fig. 3.4-Fig. 3.8 show the deflection distribution of 24 casting schemes at 1/8 cross-section, 1/4 cross-section, 3/8 cross-section, 1/2 cross-section, and vault cross-section, respectively.

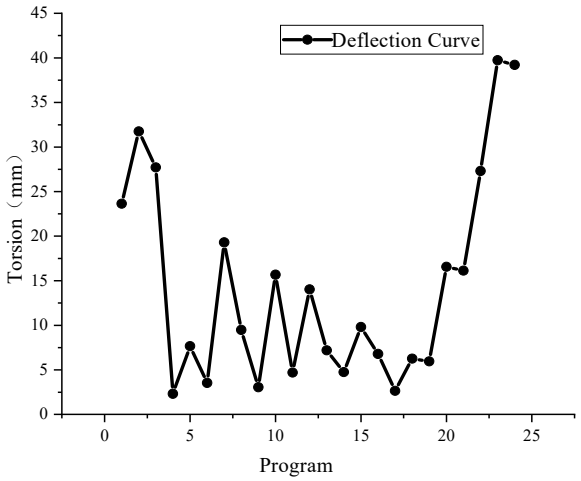

Figure 3.4 Deflection for scheme of 1/8 section

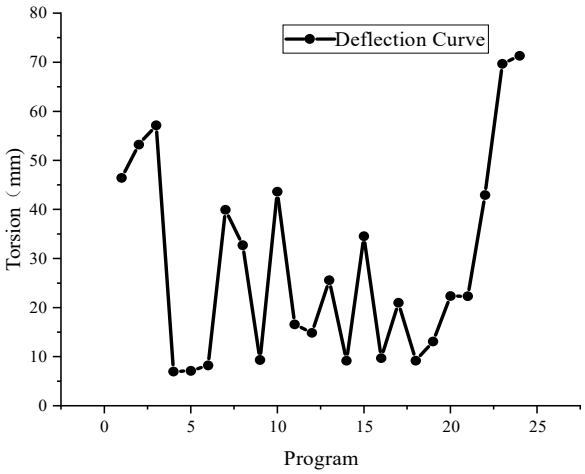

Figure 3.5 Deflection for scheme of 1/4 section

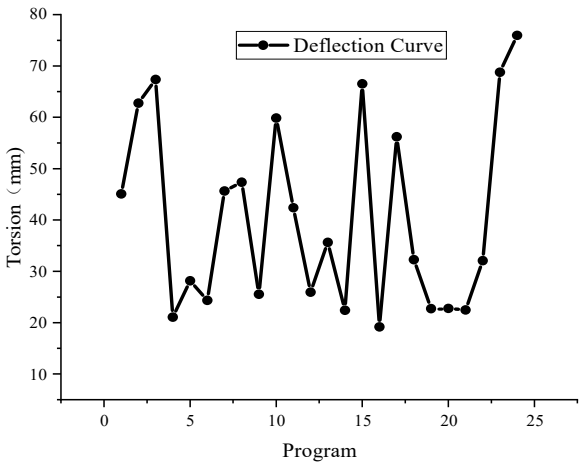

Figure 3.6 Deflection for scheme of 3/8 section

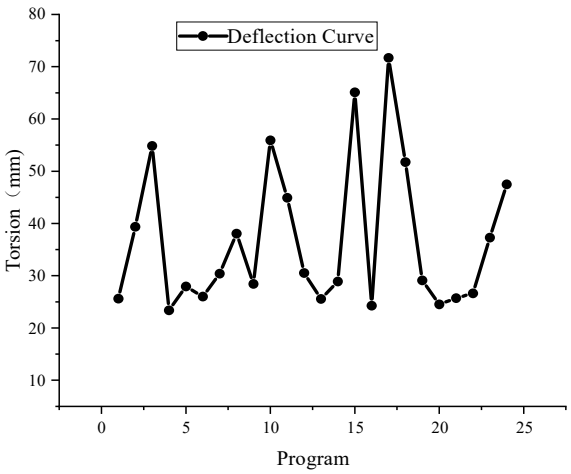

Figure 3.7 Deflection for scheme of 1/2 section

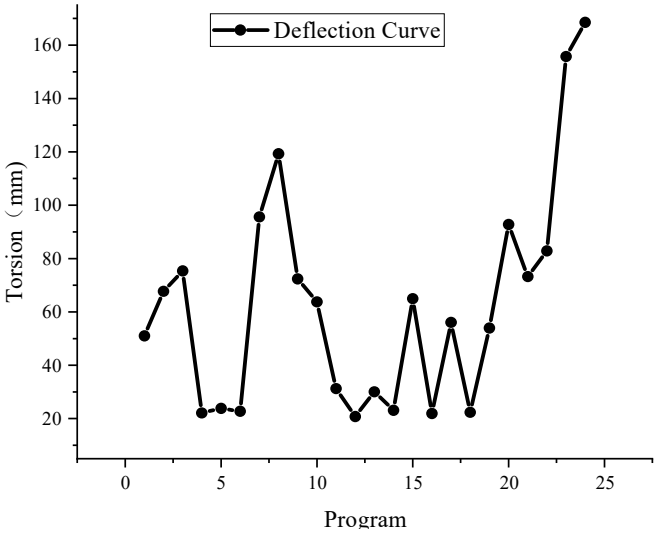

Figure 3.8 Deflection for scheme of the vault section

The results of the deflection of the cross-section of each scheme of the first pouring from Fig. 3.4 to Fig. 3.8 show that Scheme 4 (simultaneous pouring of 1-1, 3-1, 5-1 and 7-1 footings) has the most outstanding performance in terms of the overall deformation control and deflection equilibrium of each cross-section. The minimum deflection value is a key parameter to evaluate the stability of the structure, and the deflection of each section of scheme 4 is at a low level, including the deflection of the foot of the arch is 0 mm (no deformation due to the constraints), the 1/8 section is only 2.32 mm, the 1/4 section is 6.97 mm, the 3/8 section is 21.08 mm, the 1/2 section is 23.38 mm, and the top of the arch section is 22.13 mm. the maximum deflection occurs in the 1/1/2 section (23.38 mm), and the maximum deflection occurs in the 1/1/1 section (23.38 mm). 2 section (23.38 mm), which is significantly lower than the extreme values of the other schemes (e.g., the deflection of the vault reaches 168.56 mm for scheme 23 and 155.76 mm for scheme 24). In addition, the deflection distribution of Scenario 4 shows a gentle transition, and there is no local mutation or peak, for example, the difference in deflection from 3/8 to the vault section is only 1.3 mm (21.08 mm to 22.13 mm), while the difference in the same interval of Scenario 23 is as high as 87.68 mm (68.8 mm to 155.76 mm), which indicates that the stress distribution of Scenario 4 is more uniform, and the structural stress caused by excessive local deflection can be effectively avoided. The risk of structural cracking due to excessive local deformation is effectively avoided.

Comparing with other candidate solutions, although Solution 14 performs slightly better in the deflection of the vault (23.12 mm) and 1/2 section (18.89 mm), its deflection of 1/8 and 1/4 section (4.75 mm, 9.17 mm) is significantly higher than that of Solution 4 (2.32 mm, 6.97 mm), and the sum (78.36 mm) and the average value (15.67 mm) are higher. Balance is not enough. Although the deflection of 1/2 section (23.26 mm) of Scheme 16 is close to that of Scheme 4, the deflections of 1/8 and 1/4 sections (6.79 mm, 9.68 mm) are higher, and the sum reaches 80.83 mm, which further emphasizes the advantage of Scheme 4. In addition, some schemes such as schemes 23 and 24 have lower deflections in the early sections (e.g., 1/8 and 1/4), but the deflections at the vault increased abruptly to 155.76 mm and 168.56 mm, which indicates that there is a serious imbalance in the pouring sequence or load distribution, and it may lead to the instability of the structure. The deflection from the foot of arch to the top of arch increases gradually through the reasonable design of casting process, which is in line with the law of gradual increase of bending moment in the force characteristics of arch bridges, and thus improves the durability of the structure while guaranteeing the construction safety.

4. Conclusion

Based on the first pouring of concrete outside the eight working faces, the first-order flexural modal coefficient of Scheme 4 (simultaneous pouring of 1-1, 3-1, 5-1 and 7-1 bottom slabs) reaches 22.51, which is the highest value of all the schemes, indicating that its ability to resist destabilization is significantly enhanced. In contrast, the flexural modal coefficient of Option 23 (4.56) and Option 24 (6.20) was only 1/5~1/3 of that of Option 4 due to insufficient confinement of the casting section close to the vault, and there was a significant risk of instability. The deflections of Scheme 4 (simultaneous casting of 1-1, 3-1, 5-1, and 7-1 base slabs) were at the lowest level in all critical sections: 1/8 section (2.32 mm), 1/4 section (6.97 mm), 3/8 section (21.08 mm), 1/2 section (23.38 mm), and vault (22.13 mm), with maximum deflections 86% lower than those of the worst scheme (Scheme 24 vault 168.56 mm) by 86.9%.

References

[1] Bergmeister K, Capsoni A, Corradi L, et al. Lateral elastic stability of slender arches for bridges including deck slenderness[J]. Structural engineering international, 2009, 19(2): 149-154.

[2] Song F, Jia H. Numerical simulation of overall stability of concrete filled steel tube arch bridge[C]//2010 International Conference on Computer Application and System Modeling (ICCASM 2010).

[3] Xie Shangying, Qian Dongsheng. Nonlinear Stability Analysis of Stiff Skeleton Concrete Arch Bridges during Construction Phase[J]. Journal of Civil Engineering, 2000, 33(01): 23-26.

[4] Gu Anbang, Wang Rong, Liu Xiangjiang, et al. Stability study of large-span steel-tube-concrete rigid ribbed arch bridges[J]. Proceedings of the Chinese Highway Society 2001, 2001.

[5] Wu Gangruo. Nonlinear analysis of mega-span arch bridges [D]. Xi'an:Chang'an University, 2006.

[6] YANG Bingcheng, WU Gangruo, LIU Jian. Nonlinear analysis of large-span steel-tube-concrete reinforced skeleton arch bridges[J]. Bridge Construction, 2006 (1): 5-7.

[7] Chen Xiaobo. Analysis of forces and stability of large-span steel pipe concrete strong skeleton arch ribs during construction stage[J]. Chinese and foreign highways, 2015, 35(01): 134-138.